

Immunosuppressive activity of cancer-associated fibroblasts in head and neck squamous cell carcinoma

Hideyuki Takahashi¹, Koichi Sakakura¹, Reika Kawabata-Iwakawa²,
Susumu Rokudai³, Minoru Toyoda¹, Masahiko Nishiyama³, Kazuaki
Chikamatsu^{1,*}

1 Department of Otolaryngology-Head and Neck Surgery, Gunma University
Graduate School of Medicine

2 Division of Integrate Oncology Research, Gunma University Initiative for
Advanced Research

3 Department of Molecular Pharmacology and Oncology

*Corresponding author

Department of Otolaryngology-Head and Neck Surgery,

Gunma University Graduate School of Medicine

3-39-22, Maebashi, Gunma, 371-8511, Japan

Tel.: +81-27-220-8350, Fax: +81-27-220-8369

E-mail: tikamatu@gunma-u.ac.jp

Short title: Immunosuppression by CAFs

Abstract

Cancer-associated fibroblasts (CAFs) have been shown to play an important role in angiogenesis, invasion, and metastasis. In the present study, we determined whether CAFs within the tumor microenvironment (TME) in head and neck squamous cell carcinoma (HNSCC) contributed to promoting immunosuppression and evasion from immune surveillance. Six pairs of CAFs and normal fibroblasts (NFs) were established from the resected tumor tissues of patients with HNSCC. The effects of CAFs and NFs on the functions of T cells were comparatively analyzed. T-cell proliferation was suppressed more by CAFs or their supernatants than by NFs. CAFs expressed the co-regulatory molecules, B7H1 and B7DC, whereas NFs did not. The expression levels of cytokine genes, including those for *IL6*, *CXCL8*, *TNF*, *TGFBI*, and *VEGFA*, was higher in CAFs. Moreover, PBMCs co-cultured with the supernatants of CAFs preferentially induced T-cell apoptosis and regulatory T cells over those co-cultured with the supernatants of NFs. A microarray analysis revealed that the level of genes related to the leukocyte extravasation and paxillin signaling pathways was higher in CAFs than in NFs. These results demonstrated that CAFs collaborated with tumor cells in the TME to establish an immunosuppressive network that facilitated tumor evasion from immunological destruction.

Key words: cancer-associated fibroblasts; head and neck squamous cell carcinoma; immunosuppression; regulatory T cells; T-cell apoptosis

Précis

Cancer-associated fibroblasts from head and neck cancer expressed the co-regulatory molecules, preferentially induced T-cell apoptosis and Treg, and showed higher level of genes related leukocyte extravasation and paxillin signaling pathways.

Introduction

Head and neck squamous cell carcinoma (HNSCC) is a fatal malignancy that accounts for approximately 650,000 new patients every year. In spite of continual improvements in surgical techniques and the introduction of new chemotherapeutic agents and radiotherapy regimens, the five-year survival rate of HNSCC has remained unchanged for decades and is still 50% [1,2]. Therefore, further explorations of new therapeutic targets are needed in order to improve the prognosis and survival of patients with HNSCC.

Tumor tissue is composed not only of tumor cells, but also of various stromal cells, including fibroblasts, epithelial cells, endothelial cells, and immune cells, and these stroma cells contribute to tumor growth and progression. Recent findings revealed that cancer-associated fibroblasts (CAFs), one of the most abundant and active cellular components of the tumor stroma, played an important role in angiogenesis, invasion, and metastasis unlike normal fibroblasts (NFs) residing in healthy tissue [3-5].

The abundance of CAFs has been clinically correlated with poor prognosis in several malignancies, including lung [6] and colorectal cancers [7]. CAFs produce various cytokines and growth factors, such as transforming growth factor (TGF)- β , vascular endothelial growth factor (VEGF), interleukin (IL)-6, IL-8, and insulin-like growth factor (IGF), and directly or indirectly influence the behavior of malignant cells through signaling pathways mediated by these molecules [8,9]. Based on these findings, CAFs are considered to be active participants in the induction of immunosuppression and promotion of tumor evasion from immune surveillance. However, the

immunological significance of CAFs in the tumor microenvironment (TME) is not yet fully understood.

Antitumor innate and adaptive immunity comprising the cancer immune surveillance network are generally designed to survey, recognize, and eliminate tumor cells. T cells predominantly orchestrate the host immune system, and the T-cell infiltration of tumor lesions has been reported to correlate with improved prognoses in various types of cancers [10,11]. However, antitumor immunity is often down-regulated with a developing tumor due to the expansion of regulatory T cells (Treg) as well as the production of immunosuppressive factors [12-14]. Thus, human tumors are known to employ various immunosuppressive mechanisms to evade the anti-tumor activities of immune cells, and tumor evasion from immunological destruction has recently emerged as one of the hallmarks of cancer [15].

In the present study, we investigated whether CAFs within the TME contributed to tumor evasion in HNSCC which are known to be highly immunosuppressive [16]. After establishing six pairs of CAFs and NFs from the resected tumor tissues of patients with HNSCC, we performed a comparative analysis of CAFs and NFs to evaluate their ability to regulate the functions of T cells. Our results have provided novel insights into immunosuppressive mechanisms in the TME and suggest that novel therapeutic approaches targeting CAFs may benefit patients with HNSCC.

Materials and Methods

Patient samples

Tumor tissues and their normal counterparts were obtained from 6 newly diagnosed HNSCC patients (3 oral cavity cancer and 3 hypopharyngeal cancer patients) who underwent surgery at the Department of Otolaryngology-Head and Neck Surgery, Gunma University Hospital. The normal counterparts were defined by the noncancerous region at least 2 cm away from the tumor margin. Patients received no anticancer drugs or radiotherapy before surgery. All tumors were obtained according to the protocol, which was approved by the Institutional Review Board of Gunma University. All patients provided written informed consent. The tissue was soaked in DMEM (Gibco, Grand Island, NY) supplemented with 1000 units/ml penicillin, 1000 µg/ml streptomycin, and 2.5 µg/ml fungizone (all reagents from Gibco) for four hours, then washed with DMEM supplemented with 10% FCS, 100 units/ml penicillin, and 100 µg/ml streptomycin (henceforth referred to as “conditioned DMEM”). The tissue was sliced into 1- to 3-mm³ pieces under sterile conditions. These fragments were transferred into a 6-well plate with conditioned DMEM. Half of the medium was changed once or twice a week thereafter. After the sufficient outgrowth of cells, fibroblasts were removed by a treatment with TrypLE™ Express Enzyme (Gibco) and seeded into tissue culture flasks. They were analyzed by flow cytometry or real time quantitative reverse transcription polymerase chain reaction (qRT-PCR) after the sufficient outgrowth of cells. All CAFs and NFs used in this study were from less than 10 passages. Culture

supernatants were collected from semi-confluent cultures 72 hours after the medium was changed, and then centrifuged and stored at -80°C until use.

Peripheral blood mononuclear cells.

Peripheral blood mononuclear cells (PBMCs) were prepared from healthy donor blood by density gradient centrifugation on a Ficoll-Paque PLUS (GE Healthcare, Pittsburgh PA). They were stored at -80°C until use.

Flow cytometry analysis of primary fibroblast cultures.

Fibroblasts were stained with the following mouse anti-human antibodies to define the expression of fibroblast surface markers, HLA molecules, or co-regulatory molecules: phycoerythrin (PE)-CD11b/Mac-1, PE-CD34, PE-CD45, PE-CD90/Thy-1, PE- α -smooth muscle actin (α -SMA) (all reagents from R&D Systems, Minneapolis, MN), PE-HLA class I, PE-HLA-DR, PE-CD80/B7-1, PE-CD86/B7-2, PE-B7H1/PD-L1, PE-B7DC/PD-L2, or PE-B7H3 (all reagents from eBioscience, San Diego, CA), and fibroblast activation protein (FAP; unconjugated; R&D Systems). A PE-conjugated goat anti-mouse monoclonal antibody (BD Pharmingen) was used as a secondary antibody for FAP staining. A Cytotfix/Cytoperm™ Kit (BD Bioscience, San Jose, CA) was used to perform intracellular staining for PE- α -SMA. Respective immunoglobulin G (IgG) isotype-matched controls (BD Bioscience) were used as negative controls. Flow cytometry was conducted using a FACSCalibur flow cytometer (BD Bioscience) and data analysis was performed with FlowJo software (TreeStar, Ashland, OR).

Real-time qRT-PCR.

Total RNA was extracted using an RNeasy mini kit (Qiagen, Valencia, CA). Quantitative RT-PCR was performed in triplicate using a Power SYBR Green RNA-to-CT 1-Step Kit on an Applied Biosystems StepOne (Applied Biosystems, Foster City, CA). The melting curve was recorded at the end of every run to assess product specificity. Glyceraldehyde-3-phosphate dehydrogenase (*GAPDH*) was used as an internal control gene. Relative expression levels were determined by the $2^{-\Delta\Delta Ct}$ method, in which Ct represented the threshold cycle.

The PCR primers used in this study were as follows: *IL6* forward primer, 5'-AAGCCAGAGCTGTGCAGATGAGTA-3', reverse primer, 5'-TGTCCTGCAGCCACTGGTTC-3'; *CXCL8* forward primer, 5'-GTGCAGAGGGTTGTGGAGAAGTTT-3', reverse primer, 5'-TCACTGGCATCTTCACTGATTCTTG-3'; *IL10* forward primer, 5'-GAGATGCCTTCAGCAGAGTGAAGA-3', reverse primer, 5'-AGGCTTGGCAACCCAGGTAAC-3'; *TNF* forward primer, 5'-TGCTTGTTCTCAGCCTCTT-3', reverse primer, 5'-CAGAGGGCTGATTAGAGAGAGGT-3'; *VEGFA* forward primer, 5'-ACTTCCCAAATCACTGTGG-3', reverse primer, 5'-GTCACACTTTGCCCTGT-3'; *TGFBI* forward primer, 5'-AGCGACTCGCCAGAGTGGTTA-3', reverse primer, 5'-GCAGTGTGTTATCCCTGCTGTCA-3'; *FOXP3* forward primer, 5'-GTTACACACGCATGTTTGCCTTC-3', reverse primer, 5'-

GCACAAAGCACTTGTGCAGACTC-3', and *GAPDH* forward primer, 5'-GCACCGTCAAGGCTGAGAAC-3'; reverse primer, 5'-ATGGTGGTGAAGACGCCAGT-3'.

Carboxyfluorescein succinimidyl ester (CFSE)-based suppression assay.

Healthy donor PBMCs were incubated with 1.5 μ M CFSE (Molecular Probe/Invitrogen) for 15 min at 37°C and quenched with ice-cold FBS. After 5 min at room temperature in the dark, they were centrifuged and washed a further three times. CFSE-labeled PBMCs (1×10^5) were plated into 96-well plates in the presence of CAFs or NFs (2.5×10^4) or culture supernatants from CAFs or NFs (half diluted with conditioned RPMI 1640 medium). An anti-CD3/anti-CD28 stimulus (Treg Suppression Inspector human; Miltenyi Biotec, Bergisch Gladbach, Germany) was added and the incubation continued for a further 4 days. They were then harvested and washed with phosphate buffered saline (PBS) supplemented with 0.1% FBS and 0.1% NaN₃. They were stained with allophycocyanin (APC)-CD3 (BD Bioscience) and 7-amino-actinomycin D (7-AAD; BD Bioscience). The proliferation of T cells was analyzed by the dilution of CFSE staining intensity using flow cytometry. Viable T cells were gated based on positive CD3 staining and negative 7-AAD staining. For blocking experiments, anti-B7H1 mAb, anti-B7DC mAb (each 10 μ g/ml; eBioscience), anti-TGF- β neutralizing mAb, and anti-VEGF neutralizing mAb (each 10 μ g/ml; R&D Systems) were used.

T-cell apoptosis assay.

A total of 500,000 PBMCs obtained from healthy donors were plated onto 48-well plates in culture supernatants from CAFs or NFs (half diluted with conditioned RPMI 1640 medium). An anti-CD3/anti-CD28 stimulus was added and the incubation continued for a further 3 days. A CaspACE™ fluorescein isothiocyanate (FITC)-VAD-FMK *In Situ* Marker (Promega, Madison, WI, USA) was used to detect T cell apoptosis. After 3 days, PBMCs were harvested and washed with PBS supplemented with 0.1% FBS and 0.1% NaN₃, then stained with FITC-VAD-FMK according to the manufacturer's instructions. They were subsequently stained with APC-CD3 (BD Bioscience) and then analyzed by flow cytometry. Five microliters of 7-AAD was added prior to flow cytometry. T cells were gated based on positive CD3 staining.

Regulatory T cell induction assay

A total of 500,000 PBMCs obtained from healthy donors were plated onto 48-well plates in culture supernatants from CAFs or NFs (half diluted with conditioned RPMI 1640 medium). An anti-CD3/anti-CD28 stimulus was added and the incubation continued for a further 4 days. They were then harvested and washed with PBS supplemented with 0.1% FBS and 0.1% NaN₃. To detect Foxp3⁺ regulatory T cells (Tregs), cells were stained with APC-CD4 antibodies (BD Bioscience), and intracellular staining for PE-Foxp3 (eBioscience) was then performed using a Cytofix/Cytoperm™ Kit and analyzed by flow cytometry. Incubated PBMCs were harvested and washed with PBS, and analyzed according to the method described in the real-time

qRT-PCR section. The relative mRNA expression levels of *FOXP3*, *IL10*, and *TGFB1* were examined.

Microarray analysis and pathway analysis

Three (CAF1/NF1, CAF2/NF2, and CAF3/NF3) of six pairs were compared using Agilent whole human genome oligo microarrays (Agilent Technologies, Santa Clara, CA) according to the manufacturer's instructions. RNA was isolated using standard RNA extraction protocols (NucleoSpin RNA II, Macherey-Nagel, Germany), and qualified with a model of the 2100 Bioanalyzer (Agilent Technologies). All samples showed RNA Integrity Numbers of greater than 6.0 (9.9-10.0) and were subjected to microarray experiments. A hundred nanograms of the RNAs from NFs and CAFs were amplified and labeled with Cy3 and Cy5, respectively, using the Agilent low input quick amp labeling kit (Agilent Technologies). The hybridization procedure was performed according to the Agilent 60-mer oligo microarray processing protocol using the Agilent gene expression hybridization kit (Agilent Technologies). Briefly, 300 ng of the corresponding Cy3- and Cy5-labeled fragmented cRNA was combined and hybridized to the Agilent Whole Human Genome Oligo Microarray 8x60k V2, and the fluorescence signals of the hybridized Agilent oligo microarrays were detected using Agilent's DNA microarray scanner (Agilent Technologies). The Agilent Feature Extraction Software was used to read out and process the microarray image files. The commonly upregulated genes (cut-off value, $\log_{10}(\text{ratio}) > 0.5$) in the three

pairs were used for the pathway analysis using Ingenuity Pathway Analysis (IPA) software (Ingenuity Systems).

Statistical analysis

The Wilcoxon Signed-Rank Test was used to test for differences in the means between two groups. Two-sided P values < 0.05 were considered to be significant. All statistical analyses were performed using the Statistical Package for the Social Sciences version 22.0 (SPSS, Armonk, NY).

Results

Establishment of CAFs and NFs from HNSCC

Six pairs of CAFs and NFs were generated from the resected tumor samples of patients with HNSCC. These cells grew in primary cultures in an adherent fashion and possessed a fibroblast-like morphology. To confirm that these cells were fibroblasts, and not contaminated with leukocytes, endothelial cells, and tumor cells, cells were analyzed using flow cytometry. As shown in Fig. 1A, NFs and CAFs were both negative for CD11b, CD34, and CD45, and positive for CD90 and FAP, which indicated that they were not contaminated by any other cells. The levels of α -SMA expressed by CAFs were higher than those by NFs, indicating that fibroblasts prepared from tumor tissues possessed an activated phenotype. These results confirmed the identity of the cultures as CAFs and NFs for further assays.

Expression of HLA molecules and co-regulatory molecules on CAFs and NFs

The expression of HLA molecules and B7 family co-regulatory molecules was investigated to characterize the immunological phenotypes of CAFs and NF. CAFs and NFs were both positive for HLA class I, but not for HLA-DR, and the expression level of HLA class I was similar between CAFs and NFs (data not shown). As shown in Fig. 1B, CAFs and NFs were both negative for CD80, CD86, and B7H3. Furthermore, CAFs, but not NFs expressed B7H1 and B7DC on the cell surface; however, the expression level of B7H1 and B7DC on CAFs was modest.

Up-regulation of cytokine genes in CAFs

We analyzed differences in the expression levels of various cytokine genes, including *IL6*, *CXCL8*, *TNF*, *TGFBI*, and *VEGFA*, between CAFs and NFs by real-time qRT-PCR. The expression levels of the cytokine genes tested were higher in CAFs obtained from six HNSCC patients than in control NFs (Fig. 1C). Their increasing ratio of gene expression varied with each cytokine or in each case.

Inhibition of T-cell proliferation

To assess the effects of CAFs and NFs on T-cell proliferation, CAFs and NFs were co-cultured with CFSE-labeled T cells. After 4 days of being co-cultured with the anti-CD3/anti-CD28 stimulus, the proliferation of T cells was measured using flow cytometry. In co-cultures, the suppressor activity of CAFs was greater than that of NFs (Fig. 2A). In order to confirm whether CAFs suppressed T-cell proliferation in a cell contact-dependent or cytokine-dependent manner, the culture supernatant from CAFs was harvested and used instead of CAFs in the T-cell proliferation assay. As expected, the inhibition of T-cell proliferation by the culture supernatant from CAFs was higher than that from NFs (Fig. 2B). Moreover, as shown in Fig. 2C, experiments using several healthy donors showed that the suppression of T cell proliferation was significantly greater by the culture supernatant from CAFs from six HNSCC patients than by that from NFs. These results suggested that CAFs directly suppressed antitumor immune responses by producing various soluble factors including immunosuppressive cytokines.

Inhibitory mechanisms of T-cell proliferation by CAFs

Next, the potential role of co-regulatory molecules and immunosuppressive cytokines in the suppressive function of CAFs was investigated through the use of blocking and neutralizing mAbs, respectively.

As expected, addition of anti-B7H1 mAb and anti-B7DC mAb significantly restored T-cell proliferation (Fig. 3A and 3B). Thus, the suppressive effects of CAFs appear to be partially mediated by co-regulatory molecules. These results suggested that CAFs had different immunological properties to NFs. Similarly, we investigated the importance of two immunosuppressive cytokines, TGF- β and VEGF, as key molecules suppressing T-cell proliferation. To end this, we neutralized TGF- β and VEGF from supernatants of CAFs using antibodies. As shown in Fig. 3C and 3D, neutralizing TGF- β and VEGF led to an increase of proliferated T cells. These findings suggest a pivotal role of TGF- β and VEGF as soluble factors in immune suppression mediated by CAFs.

Induction of T-cell apoptosis

To further elucidate the mechanisms underlying the suppression of T cell proliferation, we investigated whether the culture supernatants obtained from CAFs and NFs induced T-cell apoptosis. Healthy donor PBMCs were cultured with supernatants from CAFs or NFs for 3 days with an anti-CD3/anti-CD28 stimulus, and were subsequently analyzed by flow cytometry. The proportions of apoptotic T cells in PBMCs co-cultured with the

supernatant from CAFs were significantly higher than those co-cultured with the supernatant from NFs (Fig. 4A and 4B).

Induction of regulatory T (Treg) cells

We compared the percentages of Treg cells in PBMCs co-cultured with supernatant obtained from CAFs or NFs. Representative dot plots of Treg cells (CD4+FOXP3+) are shown in Fig. 4C. As expected, the proportions of Treg cells in PBMCs co-cultured with the supernatant obtained from CAFs were significantly higher than those co-cultured with the supernatant from NFs (Fig. 4D). Moreover, the gene expression levels of the Treg-specific transcription factors *FOXP3*, *IL-10*, and *TGFB1* in PBMCs co-cultured with supernatant were analyzed by real-time qRT-PCR, and the expression levels of *FOXP3*, *IL10*, and *TGFB1* were higher in PBMCs co-cultured with supernatant obtained from CAFs than in those co-cultured with the supernatant from NFs (Fig. 4E). These results suggested that CAFs also indirectly suppressed antitumor immune responses by inducing Treg cells.

Microarray analysis and pathway analysis

We performed Agilent whole human genome microarray analyses with the three pairs of CAFs and NFs. Although a hierarchical cluster analysis from the three (CAF1/NF1, CAF2/NF2, and CAF3/NF3) of six pairs revealed different genetic profiles, as shown in Fig. 5A, a hundred genes that were upregulated in the three CAFs (\log_{10} ratio > 0.5) were identified (Fig. 5B). To explore the altered canonical pathways in CAFs from those in NFs, we

characterized the functional relationship between genes upregulated in CAFs in IPA. Two signaling pathways, the leukocyte extravasation and paxillin signaling pathways, have been predicted as the most significantly activated canonical pathways (Table 1).

Discussion

Antitumor immunity has been considered to play an important role in protecting against the development of malignancy. The immune system monitors and excludes tumor cells in the early phase of tumorigenesis, and fibroblasts also contribute to a growth suppressive state, while tumor cell variants show increased resistance to immune surveillance and gradually survive and proliferate. Immune responses against tumor cells in the TME were previously reported to be strongly suppressed through a dysfunction in effector cells, as well as the infiltration and expansion of immune suppressive cells, and where fibroblasts educated by tumor cells become CAFs contributing to tumorigenesis, tumor growth, and metastasis.^{5,9} Regarding the contribution of CAFs to immune evasion, Balsamo et al. demonstrated that CAFs from melanoma interfered with NK cell functions including cytotoxicity and cytokine production [17]. On the other hand, De Monte et al. reported that CAFs from pancreatic cancer induced thymic stromal lymphopoietin-dependent Th2-type inflammation [18]. In addition to these findings, we were able to demonstrate in the present study that CAFs obtained from HNSCC were of unique immunological significance, as opposed to NFs.

Our results revealed that CAFs suppressed T cell proliferation more efficiently than NFs. This suppressive activity was observed in co-cultures not only with CAFs, but also the supernatant from CAFs. To elucidate the mechanisms underlying the suppressive effects of CAFs on T-cell proliferation, we first assessed the expression of co-stimulatory and co-regulatory molecules

by CAFs and NFs. Although co-stimulatory molecules, CD80 and CD86, were not expressed by CAFs or NFs, B7H1 and B7DC were expressed by CAFs, but not by NFs. B7H1 and B7DC are both members of the B7 family, bind PD-1 on activating T cells, and are putative negative regulators for immune function. Nazareth et al. demonstrated that a subset of CAFs obtained from non-small cell lung cancer (NSCLC) constitutively expressed B7H1 and B7DC [19]. The intensity of B7H1/B7DC expression in CAFs from HNSCC was more modest than that in CAFs obtained from NSCLC. We performed blocking assays using anti-B7H1 or B7DC, and suppressive activity was significantly restored in some of pairs tested. Nazareth et al. showed that the blockade of B7H1 and/or B7DC completely reversed the inhibition of tumor-associated T-cell activation by CAFs in one of three tumors. Thus, our results and previous findings suggest that co-regulatory molecules on CAFs may partially play an important role in T-cell suppression. CAFs originally consist of a heterogeneous population of cells from various sources; therefore, the role of B7H1 and B7/DC expression in CAFs may vary depending on factors such as their functional activities, types of cancers, and immune status in the TME. Several monoclonal antibodies that target B7H1 (PD-L1), are now being developed [20,21], and the blockade of B7H1 was recently shown to produce durable tumor regression and prolonged disease stabilization in patients with advanced cancers in a phase I trial [22]. Monoclonal antibodies against co-regulatory molecules may be somewhat useful as a CAF targeted therapy.

Since CAFs suppressed T-cell proliferation in a contact-independent manner,

we investigated T-cell apoptosis and Treg induction using culture supernatants from CAFs and NFs in order to elucidate the suppression mechanisms responsible in more detail. Previous studies have so far demonstrated that CAFs produce various cytokines and/or chemokines to promote tumor cell proliferation, angiogenesis, invasion, and metastatic dissemination [9]. Several studies found that CAFs isolated from HNSCC expressed higher levels of HGF [23], TGF- β [24], IL-33 [25], CCL7 [26], and MMP [27] than their normal counterparts. We also revealed that the gene expression levels of *IL6*, *CXCL8*, *TNF*, *TGFBI*, and *VEGFA* were higher in CAFs than in NFs. Among the cytokines evaluated in the present study, TNF- α is known to be a member of cytokines that induce apoptotic cell death in T cells. Therefore, it was not unexpected to find that CAFs significantly induced T-cell apoptosis; however, difficulties have been associated with determining the exact factors involved in T-cell apoptosis due to its complicated composition. PBMCs co-cultured with the supernatant from CAFs preferentially induced Treg. Moreover, the gene expression levels of *FOXP3*, *TGFBI*, and *IL10* were elevated in PBMCs co-cultured with the supernatant from CAFs, which supported the Treg induced being functionally activated. Treg has been shown to accumulate in the TME, promote tumor growth, and down-regulate antitumor responses [28]. The differentiation of precursor T cells is regulated by a complex network of specific cytokine signals, and a certain type of Treg is known to be induced in the periphery in response to IL-2, TGF- β , and IL-10 [29]. Moreover, VEGF has been recognized as an important factor in the induction or maintenance of Treg [30]. The up-

regulation of *TGFB1* and *VEGFA* in CAFs may play an important role in the induction of Treg. In fact, restoration of T-cell proliferation by TGF- β and VEGF neutralization in the present study supports that. Mace et al. similarly demonstrated that a culture of PBMCs with pancreatic cancer-stellate cell supernatants promoted PBMC differentiation into myeloid-derived suppressor cells, which is another major subset of regulatory cells, in a STAT3-dependent manner [31]. Thus, various factors secreted by CAFs appear to act synergistically or additively to enhance immunosuppressive ability, leading to a dysfunction in effector T cells.

We also compared the gene expression profiles of CAFs and NFs using a microarray analysis. The hierarchical clustering of gene expression in CAFs than in NFs clearly showed differences between individual patients. These results suggest that the characteristics of CAFs in the TME may be regulated by various conditions, such as inflammation, hypoxia, and angiogenesis, in which CAFs exist. In order to elucidate the activated signaling pathway related to CAFs, commonly upregulated genes in the three pairs were analyzed with IPA. Although any signaling pathway related to immunosuppression was not detected in this study, we additionally found that a set of genes, the expression of which was upregulated in CAFs, were involved in the leukocyte extravasation and paxillin signaling pathways. Paxillin is one of the crucial molecules for cell-extracellular matrix adhesion and cell migration, and plays an important role in the assembly and disassembly of focal adhesions in various cells [32,33]. These activated signaling pathways in CAFs may facilitate the recruitment of various

leukocytes including immunosuppressive cells in the TME.

In summary, we established pairs of CAFs and NFs from patients with HNSCC. CAFs expressed not only the co-regulatory molecules, B7H1 and B7DC, but also preferentially induced T-cell apoptosis and Treg over NFs. Moreover, the leukocyte extravasation and paxillin signaling pathways were predicted to be the most significantly activated canonical pathways in CAFs relative to those in NFs. Thus, CAFs modulated effector T cell function in anti-tumor immune responses in direct and indirect manners. Tumor evasion from the host immune system is a major problem in immunotherapy, and CAFs may play a pivotal role in the TME by establishing an immunosuppressive network along with tumor cells and immunosuppressive cells that facilitates the activation of an immunosuppressive pathway. Accordingly, the development of novel therapeutic agents to efficiently overcome CAF-driven immunosuppression is urgently needed.

Acknowledgments

This work was supported in part by Grants-in-Aid (24791820 to KS, 25861525 to MT, 26670736 to KC) from the Ministry of Education, Culture, Sport, Science and Technology of Japan. We thank Dr. Theresa L. Whiteside for her critical reading and comments.

Conflict of Interest

The authors declare that they have no conflict of interest.

References

1. Siegel R, Naishandham D, Jemal A. (2012) Cancer statistics, 2012. *CA Cancer J Clin* 62:10-29.
2. Leemans CR, Braakhuis BJM, Brakenhoff RH. (2011) The molecular biology of head and neck cancer. *Nat Rev Cancer* 11:9-22
3. Augsten M. (2014) Cancer-associated fibroblasts as another polarized cell type of the tumor microenvironment. *Front Oncol* 4:62.
4. Franco OE, Shaw AK, Strand DW, Hayward SW. (2010) Cancer associated fibroblasts in cancer pathogenesis. *Semin Cell Dev Biol* 21:33-39.
5. Kalluri R, Zeisberg M. (2006) Fibroblasts in cancer. *Nat Rev Cancer* 6:392-401.
6. Ito M, Ishii G, Nagai K, Maeda R, Nakano Y, Ochiai A. (2012) Prognostic impact of cancer-associated stromal cells in patients with stage I lung adenocarcinoma. *Chest* 142:151-158.
7. Herrera M, Herrera A, Domínguez G, Silva J, García V, García JM, Gómez I, Soldevilla B, Muñoz C, Provencio M, Campos-Martin Y, García de Herreros A, et al. (2013) Cancer-associated fibroblast and M2 macrophage markers together predict outcome in colorectal cancer patients. *Cancer Sci* 104:437-444.
8. Zhang J, Liu J. (2013) Tumor stroma as targets for cancer therapy. *Pharmacol Ther* 137:200-215.
9. Rasanen K, Vaheri A. (2010) Activation of fibroblasts in cancer stroma. *Exp Cell Res* 316:2713-2722.
10. Zhang L, Conejo-Garcia JR, Katsaros D, Gimotty PA, Massobrio M,

- Regnani G, Makrigiannakis A, Gray H, Schlienger K, Liebman MN, Rubin SC, Coukos G. (2003) Intratumoral T cells, recurrence, and survival in epithelial ovarian cancer. *N Engl J Med* 348:203-213.
11. Pages F, Berger A, Camus M, Sanchez-Cabo F, Costes A, Molidor R, Mlecnik B, Kirilovsky A, Nilsson M, Damotte D, Meatchi T, Bruneval P, et al. (2005) Effector memory T cells, early metastasis, and survival in colorectal cancer. *N Engl J Med* 353:2654-2666.
 12. Whiteside TL. (2010) Immune responses to malignancies. *J Allergy Clin Immunol* 125:S272-283.
 13. Talmadge JE. (2011) Immune cell infiltration of primary and metastatic lesions: Mechanisms and clinical impact. *Semin Cancer Biol* 21:131-138.
 14. Poschke I, Mougiakakos D, Kiessling R. (2011) Camouflage and sabotage: tumor escape from the immune system. *Cancer Immunol Immunother* 60:1161-1171.
 15. Hanahan D, Weinberg RA. (2011) Hallmarks of cancer: the next generation. *Cell* 144:646-674.
 16. Tong CCL, Kao J, Silora AG. (2012) Recognizing and reversing the immunosuppressive tumor microenvironment of head and neck cancer. *Immunol Res* 54:266-274.
 17. Balsamo M, Scordamaglia F, Pietra G, Manzini C, Cantoni C, Boitano M, Queirolo P, Vermi W, Facchetti F, Moretta A, Moretta L, Mingari MC, et al. (2009) Melanoma-associated fibroblasts modulate NK cell phenotype and antitumor cytotoxicity. *Proc Natl Acad Sci USA* 106:20847-20852.
 18. De Monte L, Reni M, Tassi E, Clavenna D, Papa I, Recalde H, Braga M,

- Di Carlo V, Doglioni C, Protti MP. (2011) Intratumor T helper type 2 cell infiltrate correlates with cancer-associated fibroblast thymic stromal lymphopoietin production and reduced survival in pancreatic cancer. *J Exp Med* 208:469-478.
19. Nazareth MR, Broderick L, Simpson-Abelson MR, Kelleher RJ Jr., Yokota SJ, Bankert RB. (2007) Characterization of human lung tumor-associated fibroblasts and their ability to modulate the activation of tumor-associated T cells. *J Immunol* 178:5552-5562.
20. Kyi C, Postow MA. (2014) Checkpoint blocking antibodies in cancer immunotherapy. *FEBS Lett* 588:368-376.
21. Hamid O, Carvajal RD. (2013) Anti-programmed death-1 and anti-programmed death-ligand 1 antibodies in cancer therapy. *Expert Opin Biol Ther* 13:847-861.
22. Brahmer JR, Tykodi SS, Chow LQ, Hwu WJ, Topalian SL, Hwu P, Drake CG, Camacho LH, Kauh J, Odunsi K, Pitot HC, Hamid O, et al. (2012) Safety and activity of anti-PD-L1 antibody in patients with advanced cancer. *N Engl J Med* 366:2455-2465.
23. Knowles LM, Stabile LP, Egloff AM, Rothstein ME, Thomas SM, Gubish CT, Lerner EC, Seethala RR, Suzuki S, Quesnelle KM, Morgan S, Ferris RL, et al. (2009) HGF and c-Met participate in paracrine tumorigenic pathways in head and neck squamous cell cancer. *Clin Cancer Res* 15:3740-3750.
24. Rosenthal E, McCrory A, Talbert M, Young G, Murphy-Ullrich J, Gladson C. (2004) Elevated expression of TGF- β 1 in head and neck cancer-

- associated fibroblasts. *Mol Carcinog* 40:116-121.
25. Chen SF, Nieh S, Jao SW, Wu MZ, Liu CL, Chang YC, Lin YS. (2013) The paracrine effect of cancer-associated fibroblast-induced interleukin-33 regulates the invasiveness of head and neck squamous cell carcinoma. *J Pathol* 231:180-189.
 26. Jung DW, Che ZM, Kim J, Kim K, Kim KY, Williams D, Kim J. (2010) Tumor-stromal crosstalk in invasion of oral squamous cell carcinoma: a pivotal role of CCL7. *Int J Cancer* 127:332-344.
 27. Johansson AC, Ansell A, Jerhammar F, Lindh MB, Grenman R, Munck-Wikland E, Östman A, Roberg K. (2012) Cancer-associated fibroblasts induce matrix metalloproteinase-mediated cetuximab resistance in head and neck squamous cell carcinoma cells. *Mol Cancer Res* 10:1158-1168.
 28. Elkord E, Alcantar-Orozco EM, Dovedi SJ, Tran DQ, Hawkins RE, Gilham DE. (2010) T regulatory cells in cancer: recent advances and therapeutic potential. *Expert Opin Biol Ther* 10:1573-1586.
 29. Knosp CA, Johnston JA. (2012) Regulation of CD4+ T-cell polarization by suppressor of cytokine signalling proteins. *Immunology* 135:101-111.
 30. Wada J, Suzuki H, Fuchino R, Yamasaki A, Nagai S, Yanai K, Koga K, Nakamura M, Tanaka M, Morisaki T, Katano M. (2009) The contribution of vascular endothelial growth factor to the induction of regulatory T-cells in malignant effusions. *Anticancer Res* 29:881-888.
 31. Mace TA, Ameen Z, Collins A, Wojcik S, Mair M, Young GS, Fuchs JR, Eubank TD, Frankel WL, Bekaii-Saab T, Bloomston M, Lesinski GB. (2013) Pancreatic cancer-associated stellate cells promote differentiation

of myeloid-derived suppressor cells in a STAT3-dependent manner.
Cancer Res 73:3007-3018.

32. Gumbiner BM. (1996) Cell adhesion: the molecular basis of tissue architecture and morphogenesis. Cell 84:345-357.

33. Turner CE. (2000) Paxillin and focal adhesion signaling. Nat Cell Biol 2:E231-236.

Figure legends

Figure 1

Establishment of CAFs and NFs from HNSCC and their characteristics.

Flow cytometry analysis of CAFs and NFs generated from resected tumor samples of patients with HNSCC. Primary cultures of CAFs and NFs were stained with CD11b, CD34, CD45, CD90, FAP, and α -SMA. CAFs and NFs were both negative for CD11b, CD34, and CD45, and positive for CD90 and FAP. α -SMA expression levels in CAFs were higher than those in NFs. (A) Representative data from one cancer patient.

The expression of co-stimulatory and co-regulatory molecules on CAFs and NFs. Flow cytometry was performed as described in the Materials and Methods. (B) Representative data from one cancer patient. CAFs and NFs were both negative for CD80, CD86, and B7H3. The expression levels of B7H1 and B7DC in CAFs were higher than those in NFs.

Up-regulation of cytokine genes in CAFs from HNSCC patients. (C) Total RNA was extracted from the generated CAFs and NFs, and increases in the expression levels of *IL6*, *CXCL8*, *TNF*, *TGF β 1*, and/or *VEGFA* were detected by real-time qRT-PCR.

Figure 2

Suppressive activity on T-cell proliferation by CAFs and NFs.

Generated CAFs and NFs were co-cultured with CFSE-labeled T cells for 4 days with an anti-CD3/anti-CD28 stimulus. They were stained with APC-CD3 and 7-amino-actinomycin D (7-AAD) to gate viable CD3⁺ T cells. The

proliferation of T cells was analyzed by the reduction of CFSE staining intensity using flow cytometry. (A) Representative data of the proliferation of T cells cultured with CAFs or NFs. (B) Representative data of the proliferation of T cells cultured with supernatants from CAFs or NFs. (C) The suppression of T cell proliferation was significantly greater by the culture supernatant from CAFs from the six HNSCC patients tested than by that from NFs. *Asterisk* (*) indicates significant difference ($P < 0.05$) between NFs and CAFs.

Figure 3

The role of co-regulatory molecules and immunosuppressive cytokines in T-cell suppression by CAFs.

CAF5 were pretreated with anti-B7H1 mAb or anti-B7DC mAb, and then co-cultured with CFSE-labeled T cells for 4 days with an anti-CD3/anti-CD28 stimulus. The proliferation of T cells was analyzed using flow cytometry. (A) Representative data from one patient (CAF5). (B) Addition of anti-B7H1 mAb and anti-B7DC mAb significantly restored T-cell proliferation.

Similarly, CAF3 supernatants were pretreated with anti-TGF- β or anti-VEGF neutralizing mAb, and then added to CFSE-labeled PBMCs for T-cell proliferation assays. (C) Representative data from one patient (CAF3). (D) TGF- β and VEGF neutralization also significantly increased the percentage of proliferated T cells. *Asterisk* (*) indicates significant difference ($P < 0.05$) compared with control IgG.

Figure 4

Induction of T-cell apoptosis and Treg (CD4+Foxp3+) in PBMCs co-cultured with the supernatant from CAFs or NFs.

PBMCs prepared from healthy donors were cultured with the supernatant from CAFs or NFs for 3 days with an anti-CD3/anti-CD28 stimulus, and subsequently analyzed by flow cytometry. They were stained with FITC-VAD-FMK, APC-CD3, and 7-amino-actinomycin D (7-AAD), and CD3+ T cells were gated. (A) Representative data of apoptotic T cells cultured with CAFs or NFs. (B) The induction of T-cell apoptosis was significantly greater by CAFs from the six HNSCC patients tested than by NFs.

PBMCs prepared from healthy donors were co-cultured with the supernatant from CAFs or NFs for 4 days with an anti-CD3/anti-CD28 stimulus. They were stained with PE-Foxp3 and APC-CD4, and then analyzed by flow cytometry. They were also analyzed by real-time qRT-PCR after a 3-day incubation. (C) Representative data of CD4+Foxp3+Tregs in PBMCs co-cultured with the supernatant from CAFs or NFs. (D) The induction of T reg was significantly greater by CAFs from the six HNSCC patients tested than by NFs. (E) The expression levels of Treg-related genes including *FOXP3*, *TGFB1*, and *IL10* in PBMCs co-cultured with the supernatant from CAFs was higher than those co-cultured with the supernatant from with NFs. *Asterisk* (*) indicates significant difference ($P < 0.05$) between NFs and CAFs.

Figure 5

Microarray analyses with the three pairs of CAFs and NFs.

(A) Cluster diagram of a microarray analysis from three pairs of NFs and CAFs. The color bar estimates relative expression levels: Red indicates higher than average expression and blue indicates lower than average expression. (B) A list of commonly upregulated genes in CAFs obtained from three patients with HNSCC. A total of one hundred genes were identified as commonly upregulated genes from the microarray analysis between NFs and CAFs. The cut-off value of the log₁₀ (ratio) was set to be greater than 0.5.

Figure 1.

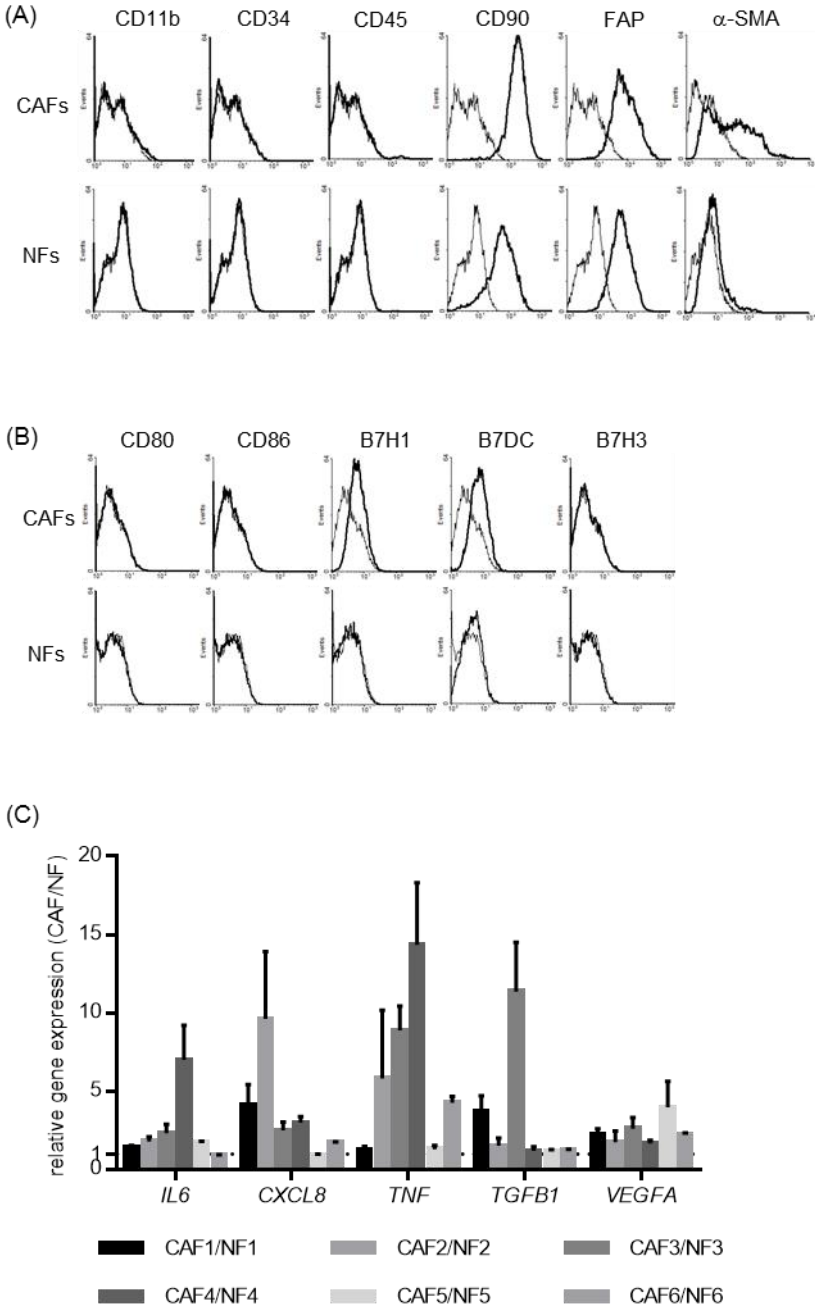


Figure 2.

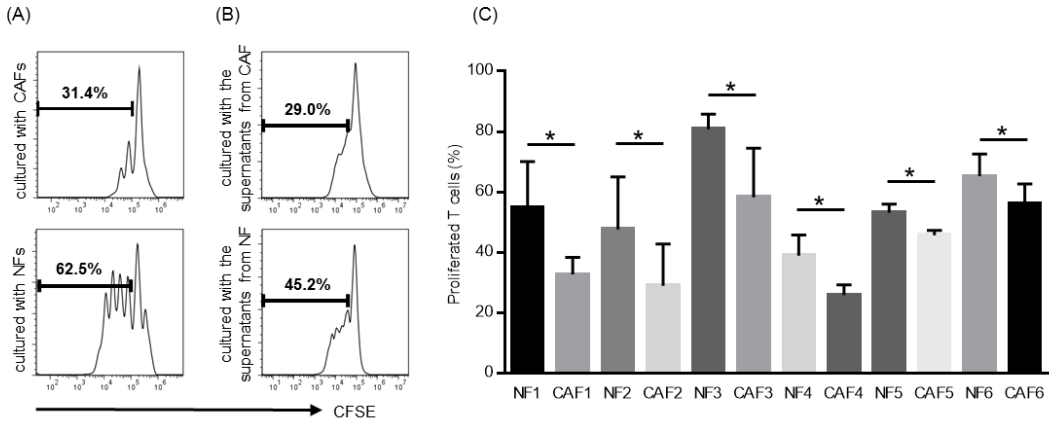


Figure 3.

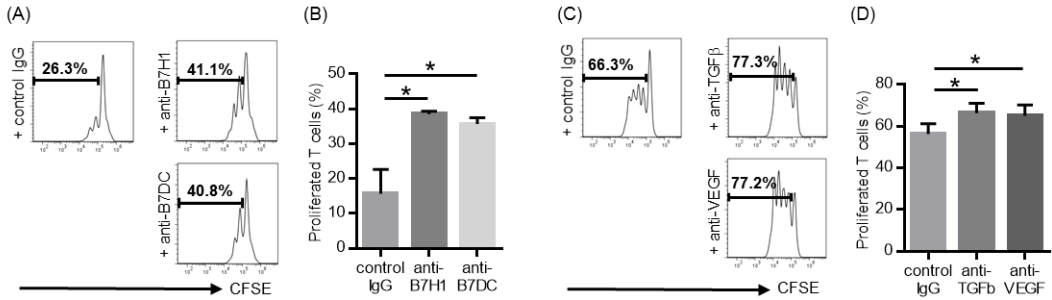


Figure 4.

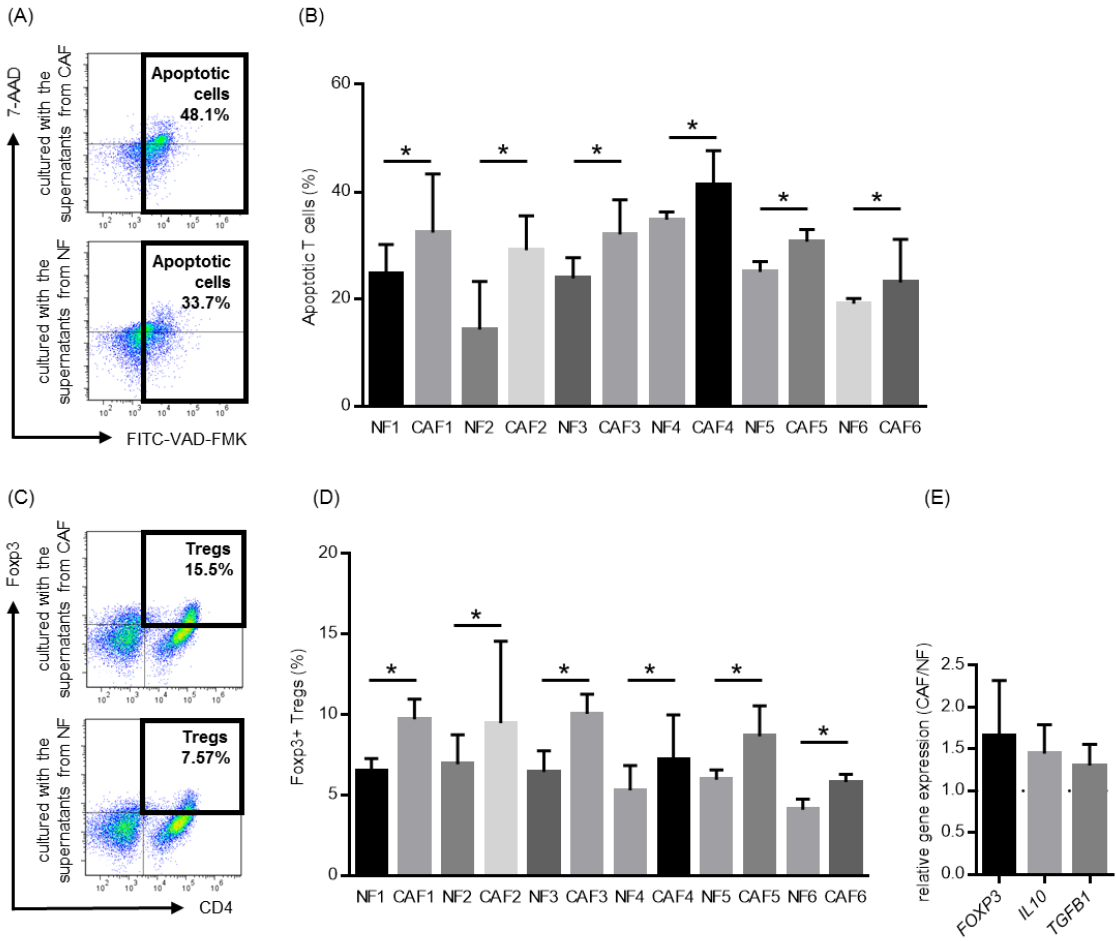
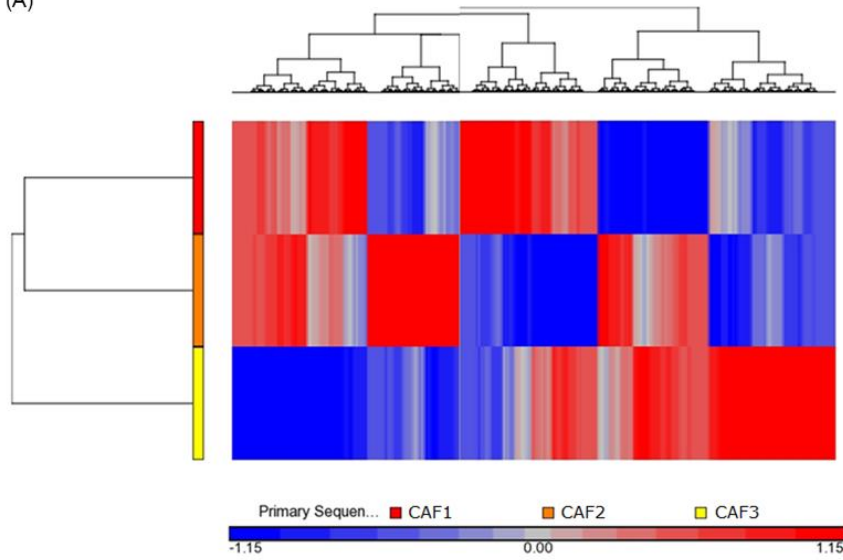
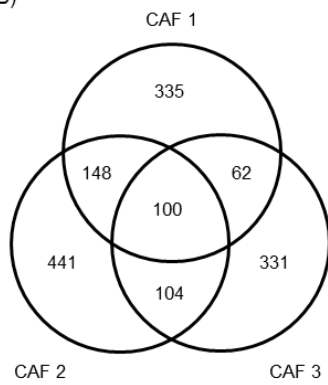


Figure 5.

(A)



(B)



| | | | | |
|-------------------|-----------------|------------------|------------------|------------------|
| <i>ST6GALNAC5</i> | <i>IL17F</i> | <i>PDZRN4</i> | <i>MBOAT1</i> | <i>PROC</i> |
| <i>NFE2L3</i> | <i>BST2</i> | <i>COL8A1</i> | <i>TFAP2A</i> | <i>NXPH2</i> |
| <i>APCDD1</i> | <i>RAB38</i> | <i>DMD</i> | <i>CD163L1</i> | <i>PLCB4</i> |
| <i>TNFSF4</i> | <i>TRPA1</i> | <i>GPR65</i> | <i>ADAMTS12</i> | <i>SLC24A4</i> |
| <i>WFDC1</i> | <i>STRA6</i> | <i>FAM169A</i> | <i>PAGE3</i> | <i>RNF144B</i> |
| <i>VAT1L</i> | <i>MAMDC2</i> | <i>COLEC10</i> | <i>CLDN18</i> | <i>MIR143HG</i> |
| <i>SLC24A3</i> | <i>OR10A7</i> | <i>MC5R</i> | <i>VWC2L</i> | <i>VPREB3</i> |
| <i>RUNX3</i> | <i>NEDD9</i> | <i>OR9G4</i> | <i>PSG1</i> | <i>KIAA0408</i> |
| <i>LEF1</i> | <i>ITGA1</i> | <i>SGIP1</i> | <i>CLDN1</i> | <i>ITGA4</i> |
| <i>C7orf69</i> | <i>TMEM176B</i> | <i>PYY</i> | <i>GREB1L</i> | <i>STYK1</i> |
| <i>COL10A1</i> | <i>B3GALT2</i> | <i>DMRT1</i> | <i>LINC00483</i> | <i>FRY</i> |
| <i>BEX1</i> | <i>ELOVL2</i> | <i>LINC00460</i> | <i>PSG8</i> | <i>NRXN1</i> |
| <i>EFNB2</i> | <i>CHN1</i> | <i>RASGRP1</i> | <i>FOLH1</i> | <i>PNKD</i> |
| <i>NTF3</i> | <i>AZU1</i> | <i>CLEC1A</i> | <i>CD8A</i> | <i>LINC00161</i> |
| <i>FAM155A</i> | <i>MMP1</i> | <i>HCLS1</i> | <i>TNS3</i> | <i>LRRC38</i> |
| <i>HSPA2</i> | <i>PADI1</i> | <i>MRVI1</i> | <i>SHROOM2</i> | <i>BCL11B</i> |
| <i>PTPRB</i> | <i>MMP3</i> | <i>A2M</i> | <i>LYPD6</i> | <i>H2AFB3</i> |
| <i>RASEF</i> | <i>SNCAIP</i> | <i>FRZB</i> | <i>CNN1</i> | <i>AGAP6</i> |
| <i>OXTR</i> | <i>DKK2</i> | <i>ANGPT1</i> | <i>FGF1</i> | <i>LINC00862</i> |
| <i>EML5</i> | <i>FAM84A</i> | <i>FAM101A</i> | <i>PIK3R3</i> | <i>RGCC</i> |